

Published in final edited form as:

*Inorg Chem.* 2013 January 7; 52(1): 77–83. doi:10.1021/ic301175f.

## Embedding the Ni-SOD mimetic Ni-NCC within a polypeptide sequence alters specificity of the reaction pathway

 Mary E. Krause<sup>1</sup>, Amanda M. Glass<sup>2</sup>, Timothy A. Jackson<sup>\*,2</sup>, and Jennifer S. Laurence<sup>\*,1</sup>
<sup>1</sup>Department of Pharmaceutical Chemistry, University of Kansas, Lawrence, KS 66047

<sup>2</sup>Department of Chemistry, University of Kansas, Lawrence, KS 66045

### Abstract

The unique metal abstracting peptide (MAP) asparagine-cysteine-cysteine (NCC) binds nickel in a square planar 2N:2S geometry and acts as a mimic of the enzyme nickel superoxide dismutase (Ni-SOD). The Ni-NCC tripeptide complex undergoes rapid, site-specific chiral inversion to DLD-NCC in the presence of oxygen. Superoxide scavenging activity increases proportionally with the degree of chiral inversion. Characterization of the NCC sequence within longer peptides with absorption, circular dichroism (CD), and magnetic CD (MCD) spectroscopies and mass spectrometry (MS) shows that the geometry of metal coordination is maintained, though the electronic properties of the complex are varied to a small extent due to bis-amide, rather than amine/amide, coordination. In addition, both the Ni-tripeptides and Ni-pentapeptides have a  $-2$  charge. The study here demonstrates that the chiral inversion chemistry does not occur when NCC is embedded in a longer polypeptide sequence. Nonetheless, the superoxide scavenging reactivity of the embedded Ni-NCC module is similar to that of the chirally inverted tripeptide complex, which is consistent with a minor change in reduction potential for the Ni-pentapeptide. Together, this suggests that the charge of the complex could affect the SOD activity as much as a change in primary coordination sphere. In Ni-NCC and other Ni-SOD mimics, changes in chirality, superoxide scavenging activity, and oxidation of the peptide itself all depend on the presence of dioxygen or its reduced derivatives (*e.g.*, superoxide), and the extent to which each of these distinct reactions occurs is ruled by electronic and steric effects that emanate from the organization of ligands around the metal center.

### Keywords

chiral inversion; Ni-NCC; MAP; nickel; bis-amide; nickel superoxide dismutase

### Introduction

The metal abstraction peptide (MAP) is a tripeptide of the sequence NCC that is capable of reacting with a metal ion to form a metal-peptide complex<sup>1,2</sup> in which the metal is coordinated in *cis* 2N:2S square planar geometry. In NCC, the sulfur ligands derive from the cysteine side chains, one amino nitrogen ligand is from the N-terminus, and one amido nitrogen ligand is from the peptide backbone.<sup>1</sup> Our previous studies on the tripeptide complex revealed that it is a structural and functional mimic of nickel superoxide dismutase (Ni-SOD) and that site-specific chiral inversion of the first (Asn) and third (Cys) residues is

\*Authors to whom correspondence should be addressed: Jennifer S. Laurence: Telephone (785) 864-3405; Fax (785) 864-5736; laurencj@ku.edu Timothy A. Jackson: Telephone (785) 864-3968; Fax (785) 864-5396; taj@ku.edu.

**Supporting Information Available:** Titration of GGNCC with nickel, CD aging profiles, CD and NMR spectra of D-containing pentapeptides, and representative CV and IR data. This information is available free of charge via the Internet at <http://pubs.acs.org>.

vital to this observed activity.<sup>2</sup> While nickel is incorporated into the peptide composed of all L amino acids, over a period of hours to days in the presence of oxygen, LLL-NCC is converted to DLD-NCC.<sup>3</sup> This chiral inversion is critical for the observed superoxide scavenging activity, as conversion from the LLL to DLD form may position the asparagine side chain to allow for substrate access to the unoccupied axial site of the metal center. Cyanide, a structural mimic of superoxide, only binds to aged Ni-NCC, suggesting a fifth ligand can only coordinate to the metal center in the chirally inverted, or DLD, form of the tripeptide-metal complex. Additionally, electrochemical studies demonstrated that the expected midpoint potential is only observed after chiral inversion occurs, and superoxide scavenging activity of the complexes increases with chiral inversion.<sup>2</sup> When the tripeptide sequence is incorporated into a longer sequence, such as a pentapeptide, metal is incorporated in a similar fashion, where the cysteinyl sulfur and backbone nitrogen ligands coordinate the metal. Although the same nitrogens bind nickel in the longer peptides, the first nitrogen is embedded in a peptide bond, resulting in amide, rather than terminal amine coordination.

Peptide maquettes and other peptide-based mimics of Ni-SOD have provided an excellent, simplified way to examine the reactivity of the enzyme, as individual components that contribute to reactivity can be modified.<sup>4-10</sup> Interestingly, no chiral inversion has been observed in Ni-SOD<sup>11-13</sup> or reported for peptide maquettes;<sup>4-6</sup> however, differences in the primary coordination sphere, such as the presence of a fifth ligand or amine/amide versus bis-amide coordination, have been shown to impact the SOD reactivity of the metal center. The nickel maquettes derived from the parent enzyme or synthetic nickel complexes that structurally mimic the Ni-SOD active site demonstrate that small differences about the metal center can lead to changes in catalysis, stability of the nickel complex, and redox potential.<sup>5,14-19</sup> While the Ni-SOD enzyme exhibits much greater activity and specificity for the superoxide scavenging activity, both the synthetic small molecule and peptide maquettes exhibit reduced function and are prone to oxidative side reactions. Ni-NCC is exceptionally stable and does not undergo oxygen-dependent degradation.; however, Ni-NCC can utilize oxygen species to perform two separate chemistries. In the presence of oxygen, site-specific chiral inversion is the dominant electron transfer pathway and precedes superoxide-scavenging activity. This inversion results in a complex with activity comparable to other peptide mimics.<sup>1-3</sup> Here we compare the differences in reactivity of the Ni-NCC tripeptide alone to Ni-NCC embedded within longer sequences, to examine the importance of chiral inversion to superoxide scavenging activity.

## Experimental

### Generation of metal-peptide complexes

The peptides GGNCC, GGGCC, GNNCC, and GNGCC, as well as GGNCC with D-cysteine in the fifth position (XXLLD-GGNCC), GGNCC with D-asparagine in the third position and D-cysteine in the fifth position (XXDLD-GGNCC), and GGNCC with D-cysteine in the fourth position (XXLDL-GGNCC), and GGNCC with D-asparagine in the third position and D-cysteine in the fourth position (XXDDL-GGNCC), were purchased from Genscript Corporation (Piscataway, NJ, USA). The X represents an achiral residue (glycine). Nickel-polypeptide complexes were generated in 50 mM potassium phosphate at pH 7.4 by adding one equivalent of NiSO<sub>4</sub>.<sup>1,2</sup>

### Circular dichroism (CD) and absorption studies

Ni-peptide samples were placed in a cuvette with a 1-cm path length and scanned from 12 500 – 33 333 cm<sup>-1</sup> (800-300 nm) using both absorption and CD spectroscopy. Samples were scanned immediately after generation and then subsequently monitored at various time

points. Background scans of buffer alone were subtracted from each scan. Absorption studies were performed on an Agilent 8453 UV/Visible spectrophotometer. Circular dichroism analysis was performed on a J-815 (Jasco Corporation) spectropolarimeter.

### Deconvolution of CD and absorption data

Deconvolution of CD and absorption data was performed using Igor Pro (Wavemetrics). Iterative Gaussian deconvolutions were performed using a minimum number of Gaussian bands. Absorption band energies were kept within 10% of the corresponding CD bands due to the broad nature of the absorption spectrum.

### Electrospray ionization mass spectrometry (ESI-MS)

Samples of Ni-GGGCC, Ni-GGNCC, Ni-GNNCC, and Ni-GNGCC were diluted 100x in a 1:1 mixture of methanol/water and analyzed on an LCT Premier (Waters Corporation) operating in negative ion mode, as described previously.<sup>1,2</sup>

### Magnetic circular dichroism (MCD)

Samples containing 3 mM Ni-GGNCC were prepared in 50 mM phosphate at pH 7.4. An equal volume of glycerol was added, yielding a 50% glycerol solution containing 1.5 mM Ni-GGNCC. The sample was placed in an MCD cell and flash frozen. Spectra were collected on a J-815 (Jasco Corporation) interfaced with an Oxford Spectromag 4000 at +7 and -7 Tesla, and the difference was found via subtraction in order to remove any CD signal. Spectra were collected at 20, 8, and 4.5 K, and analyzed to identify any changes in the spectra that indicate paramagnetic character. The feasibility of correlating these low temperature data with the structure of Ni-GGNCC at room temperature is demonstrated by the lack of apparent changes in the corresponding CD spectra collected at 298 and 4.5 K.

### Preparation of nickel-released samples for nuclear magnetic resonance (NMR)

Ni-GGNCC was generated via spiking 3 mM GGNCC in 50 mM potassium phosphate at pH 7.4 with 1 equivalent of NiSO<sub>4</sub>. Because the metal bound form of the peptide is not compatible with standard <sup>1</sup>H NMR, presumably due to a transient paramagnetic component during reactivity, the pH was dropped to approximately 5.0 by the addition of 1M HCl to release the metal. The sample was purified using reverse-phase HPLC on a Luna 5 $\mu$  C18(2) column (Phenomenex) to remove the released nickel and to isolate the apo, nickel-exposed peptide sample (nickel-exposed GGNCC). Fractions containing nickel-exposed GGNCC were pooled and lyophilized.

### NMR

Peptide samples (XXLLL-, XXLLD-, XXDDL-, XXLDL-, XXDLD-GGNCC, as well as nickel-exposed GGNCC) were dissolved at a concentration of 3 mM in 50 mM potassium phosphate, pH 7.4, containing 10% D<sub>2</sub>O. <sup>1</sup>H spectra were acquired using a 500 MHz Bruker DRX spectrometer equipped with a triple resonance probe. Water suppression was accomplished using presaturation.

### Ni-SOD xanthine/xanthine oxidase coupled assay

Superoxide scavenging activity was determined as reported previously,<sup>1</sup> except Ni-peptides were generated *in situ* using one equivalent of NiSO<sub>4</sub>. In brief, xanthine/xanthine oxidase generates superoxide. Reaction of superoxide with cytochrome *c* is detected by an increase in absorbance at 550 nm. Introduction of a superoxide scavenger slows this reaction, resulting in lower absorbance. Adding different amounts of the superoxide-scavenging molecule leads to generation of an IC<sub>50</sub> curve, where smaller IC<sub>50</sub> values indicate higher superoxide scavenging activity. Superoxide scavenging activity of Ni-GGGCC, Ni-GGNCC,

Ni-GNNCC, and Ni-GNGCC was determined using the standard xanthine/xanthine oxidase method developed by Crapo and coworkers.<sup>20</sup> All reagents were generated in 50 mM potassium phosphate, 100  $\mu$ M EDTA reaction buffer at pH 7.8 except for the Ni-peptide complexes, which were generated in 50 mM potassium phosphate, pH 7.4. In this assay, 600  $\mu$ M cytochrome *c* from bovine heart (Sigma), 300  $\mu$ M xanthine (Sigma) and enough xanthine oxidase from buttermilk (Sigma) to cause a change in absorbance at 550 nm of 0.02 – 0.04 AU per minute were added to a final volume of 300  $\mu$ L with reaction buffer. The change in absorbance at 550 nm was monitored on a Cary 100 UV-Visible spectrophotometer (Varian).

### Electrochemistry

Electrochemical data were collected as previously described.<sup>1</sup> 3-mL samples of 3 mM Ni-GGNCC and Ni-GGGCC were prepared in 50 mM potassium phosphate at pH 7.4. After incorporation, pH was raised to 10. Cyclic voltammetry (CV) data were collected with a CH1812C Electrochemical Analyzer potentiostat (CH Instruments) with a three-electrode setup (platinum working electrode, Bioanalytical Systems, Inc.; Pt auxiliary electrode; Ag/AgCl reference electrode) in a glass CV cell. Potential was applied from zero to 1.2 V with a scan rate of 0.2 V per second, and current was measured.

### Coordination of cyanide and infrared spectroscopic (IR) analysis

Samples of Ni-GGGCC and Ni-GGNCC were prepared at a concentration of 3 mM in 50 mM potassium phosphate at pH 7.4. One equivalent of potassium cyanide was added to each of the samples. Samples were flash frozen and lyophilized. IR analysis was performed to observe the cyanide peak in each sample. IR spectra were acquired from dry powder samples on a Perkin Elmer Spectrum 100 FT-IR spectrometer equipped with a universal ATR (Attenuated Total Reflection) sampling accessory. The spectrum of solid potassium cyanide was used to compare the shift of  $\nu(\text{C}\equiv\text{N})$  vibration from the free to the nickel-coordinated state.

### Electronic paramagnetic resonance (EPR)

Samples of Ni-GGNCC were prepared at a concentration of 2 mM in 50 mM potassium phosphate at pH 7.4. One equivalent of potassium cyanide was added to one sample. The solutions were placed into EPR tubes and immediately flash frozen in liquid nitrogen. X-band electronic paramagnetic resonance (EPR) experiments were performed on a Bruker EMXplus spectrometer. These sets of experiments were performed at 77 K and the following range of parameters were employed: microwave frequency = 9.63 GHz; microwave power = 3.6 – 7.9 mW; modulation amplitude: 8.0 G; modulation frequency = 100.0 kHz; and time constant = 10.24 – 81.92 ms, which are similar to those used previously for peptide maquettes.<sup>9</sup>

## Results

### Preparation and spectroscopic characterization of Ni-peptides

The NCC tripeptide sequence was incorporated into a series of four pentapeptides (GGNCC, GGGCC, GNNCC, and GNGCC). As previously reported,<sup>1,2</sup> metal incorporation in the appropriate geometry occurs via metal transfer from a weaker chelating moiety. While immobilized metal affinity chromatography resin has been an ideal choice for obtaining pure compounds for examination following the metallation reaction, for studies requiring immediate spectroscopic analysis, a solution transfer is preferred. Although  $\text{NiCl}_2$  fails to generate the desired complex,  $\text{NiSO}_4$  enables metal incorporation and provides the same spectral features without the need for a solid support. The peptides were analyzed with CD

spectroscopy to validate the ligands involved in the metal coordination. The spectral features were slightly different than those previously reported for the non-chirally inverted Ni-NCC tripeptide,<sup>3</sup> which is expected because the amine nitrogen ligand from the N-terminus in the tripeptide is replaced by an amide nitrogen ligand in the longer peptides. The four pentapeptides have identical spectral profiles, with only very minor differences in intensity (Figure 1). Absorbance and CD spectra of Ni-GGNCC were deconvoluted using a minimum number of Gaussian bands, in order to provide a quantitative comparison to the amine/amide Ni-NCC species (Figure 2 and Table 1).<sup>3</sup> MS data reveal the Ni complex of each pentapeptide is at the expected mass (e.g. Ni-GGNCC,  $m/z = 506.22$ , calculated = 506.02), and a nickel titration supports the 1:1 metal to peptide ratio (Figure S1). Nickel was also incorporated into analogous peptides that have been extended at the C-terminus as well as whole proteins, yielding absorption, CD, and MS results comparable to the pentapeptide data (data not shown); this indicates extension of the C-terminus does not impede binding. Taken together, these data indicate that the metal is coordinated 2N:2S with two amide backbone nitrogens and two cysteine side chains (Figure 3), which is very similar to coordination of the nickel tripeptide complex reported previously. The overall charge on the complex is  $-2$ , the same as that of Ni-NCC, despite the change to bis-amide coordination in the Ni-pentapeptides.

In the case of the Ni-NCC tripeptide complex, the nickel ion is primarily Ni<sup>II</sup>;<sup>1</sup> however, it was considered that change from amine/amide coordination in the tripeptide to the bis-amide coordination in the pentapeptide may stabilize a Ni<sup>III</sup> state, leading to a mixture of Ni<sup>II/III</sup> forms. To test for the presence of Ni<sup>III</sup>, MCD and EPR data were collected on the Ni-GGNCC sample. Ni<sup>III</sup> was not observed in X-band EPR experiments performed at 77 K using standard conditions (data not shown). In addition, MCD spectra collected at 7 T in the near-IR and visible regions (800 – 300 nm) show no temperature dependence over the range of 4.5 to 25 K, which indicates no paramagnetic components with electronic transitions in the visible to near-UV spectral region are detectable (data not shown), further suggesting that Ni<sup>III</sup> does not accumulate.

### Circular dichroism analysis of Ni-pentapeptide complexes containing D amino acids

In the NCC tripeptide, chiral inversion occurs at the first and third positions, where nickel incorporated into LLL-NCC mediates the conversion to the DLD-NCC isoform over the course of hours. This chiral inversion is apparent in the CD spectra, as the signs of the DLD-NCC peaks are opposite of those of the LLL-NCC.<sup>2</sup> With the pentapeptide complex, however, following the insertion reaction, changes in sign are not observed in the CD spectra, but only a small decrease in intensity occurs on this timescale (Figure S2). As such, the lack of sign change suggests chiral inversion either does not occur or it occurs on a much faster timescale than in the tripeptide, such that changes in spectral features cannot be observed by CD.

To further explore the possibility of chiral inversion in the pentapeptide and identify any affected position(s), the pentapeptides XXLDL-GGNCC, XXLLD-GGNCC, XXDLLD-GGNCC and XXDDL-GGNCC were metallated and the CD spectra of the resulting Ni<sup>II</sup> complexes were compared to the all-L isoform (Figure 4). The spectra of the Ni-bound D-amino acid-containing peptides are all different from that observed for the all-L form of Ni-GGNCC, suggesting chiral inversion likely does not occur in the pentapeptide complex. Specifically, the XXDLLD- and XXLLL-GGNCC nickel complexes have spectra that are nearly mirror images of one another; since DLD-NCC is the final form of the tripeptide complex, this indicates the bis-amide pentapeptide complex and the mixed amine/amide tripeptide complex behave differently with respect to chiral inversion chemistry.

## Nuclear magnetic resonance of chiral forms of the pentapeptides

To validate the absence of chiral inversion in the Ni-pentapeptide system,  $^1\text{H-NMR}$  data were collected for a set of control peptides.  $^1\text{H-NMR}$  spectra were acquired for the apo forms of the all-L, XXDDL, XXDL, XXLDL, and XXLLD-GGNCC systems to assess differences in splitting patterns for species containing D-amino acids. To determine which form the nickel-exposed GGNCC resembles, a sample of GGNCC was metallated, the pH was dropped to release the metal, and the peptide was separated from free nickel using reverse phase HPLC. After purification and isolation of the nickel-exposed GGNCC, NMR was employed, and the spectrum of the nickel-exposed GGNCC was compared to that of each GGNCC form. The spectra of the peptides are very similar, with modest differences between 2.65 and 3.0 ppm (Figure 5 and S3-S7). These peaks correspond to the  $\text{CH}_2$  groups on the Asn and Cys side chains, and their splitting patterns have subtle differences that reflect changes in spatial orientation, which vary with the D or L configuration of each residue. The XXDL and XXLDL are similar to one another, and the XXLLD and XXDDL are similar to one another, which is logical based on the exact opposite chiralities of these peptides. XXLLL GGNCC and nickel-exposed GGNCC exhibit nearly identical NMR spectra, suggesting nickel-exposed GGNCC maintains its XXLLL configuration and chiral inversion does not occur in the pentapeptide.

## Reactivity of pentapeptides: Superoxide scavenging, coordination of fifth ligand, and electrochemistry

The consequences of chiral inversion for the Ni-NCC tripeptide include the ability of the complex to i) coordinate a fifth ligand ( $\text{CN}^-$ ), ii) display a measurable midpoint potential, and iii) exhibit enhanced superoxide scavenging activity. Because the Ni-pentapeptide complexes do not undergo chiral inversion, possibly due to the bis-amide coordination rather than mixed amine/amide coordination found in the tripeptide systems, it was of interest to probe these three properties of the pentapeptide complex. The xanthine/xanthine oxidase assay was performed, coordination of  $\text{CN}^-$  was monitored with CD and IR, and electrochemical studies were performed using CV.

The aged Ni-NCC tripeptide, which corresponds to the chirally inverted form, has superoxide scavenging activity ( $\text{IC} = 4.1 \times 10^{-5} \text{ } 50 \text{ M}$ ).<sup>1,2</sup> Despite having bis-amide 2N:2S coordination, the Ni-pentapeptide complexes have superoxide scavenging activity only slightly increased relative to the Ni-NCC tripeptide complex ( $\text{IC}_{50} = 9.1 \pm 5 \times 10^{-6} \text{ M}$  for Ni-GGNCC).

Cyclic voltammetry was used to measure the midpoint potential of the Ni-pentapeptides. The Ni-GGGCC and -GGNCC peptides have similar quasi-reversible potentials (respectively, 0.78 and 0.80 mV vs Ag/AgCl at pH 10; see Figure S8 for a representative scan). These values are slightly higher than those reported for the chirally inverted Ni-NCC tripeptide complex (0.71 mV vs Ag/AgCl).<sup>1</sup> Interestingly, despite not undergoing chiral inversion, the Ni-pentapeptide signal can be measured immediately after generation, whereas the tripeptide does not have a measurable potential until it has aged and therefore chirally inverted. The small difference in redox potential for the different systems is not unexpected given the compounds share similar, but not identical, coordination geometries.<sup>19</sup> While the change in coordination environment from the amine/amide-ligated Ni-NCC to the bisamide-ligated Ni-pentapeptide might be expected to cause a negative shift in the reduction potential for the latter species, this is likely not observed because these complexes have the same overall charged state (-2).

To determine if  $\text{CN}^-$  has access to bind the metal within the pentapeptide complexes, the pentapeptide complexes Ni-GGNCC and Ni-GGGCC were generated, and solid phase IR

data were collected on free cyanide and cyanide in the presence of the Ni-pentapeptide complexes (Figure S9). For the latter samples, the vibration of  $\text{CN}^-$  is shifted and corresponds to Ni-bound  $\text{CN}^-$  (Table 2), as was observed previously with the tripeptide complex, suggesting that  $\text{CN}^-$  is able to coordinate to the nickel-pentapeptide complex immediately after metal insertion.

## Discussion

The peptide sequence NCC is capable of coordinating nickel in a 2N:2S geometry, where the sulfur ligands come from the cysteine side chains, one amino nitrogen ligand is from the N-terminus, and one amido nitrogen ligand is from the peptide backbone. After metal is incorporated into the tripeptide composed of all-L amino acids, LLL-NCC is converted predominantly to DLD-NCC within hours. After this site-specific chiral inversion, the Ni-tripeptide complex shows enhanced nickel superoxide dismutase activity. Chiral inversion of this tripeptide is critical for the superoxide scavenging activity, as conversion from the LLL to DLD correlates directly with activity.<sup>2</sup>

The tripeptide sequence may be incorporated into a longer sequence without disrupting metal complex formation. Here, we examined the coordination of nickel by the NCC sequence within a series of polypeptides. ESI-MS confirms monomeric incorporation of nickel into each pentapeptide, and MCD and EPR show a lack of paramagnetic nickel(III), as is the case in the tripeptide. The CD spectral features differ from those of the all-L tripeptide, which can be observed only in the absence of oxygen.<sup>3</sup> The transitions in the pentapeptide complex are shifted to higher energy because the amine nitrogen ligand from the N-terminus in the tripeptide is replaced by an amide in the pentapeptides. The extinction coefficients observed for the electronic transitions of  $\text{Ni}^{\text{II}}$ -GGNCC are also reduced relative to those of  $\text{Ni}^{\text{II}}$ -NCC, which is most likely also reflective of the structural differences between these complexes. Importantly, the electronic absorption and CD spectra observed for the Ni-pentapeptides are nearly identical in both sign and intensity to those of the Ni-SOD<sup>M1</sup>-Ac maquette reported by Shearer and co-workers, which also contained a bis-amide ligated  $\text{Ni}^{\text{II}}$  center.<sup>5</sup> These data together indicate that the ligating moieties are analogous; the same two cysteinyl sulfur and backbone nitrogen ligands are utilized, but the extension at the N-terminus changes the nitrogen coordination from mixed amine/amide to bis-amide. The similarity of four pentapeptides, with and without asparagine present in position 3, confirms that the asparagine side chain is not directly involved in metal coordination and nitrogen ligation is due solely to the backbone amides. In the tripeptide the rate of chiral inversion can be monitored because a change in spectral features is clearly observed over time, but no observable changes occur within the pentapeptide. Examination of several chiral permutations of the GGNCC pentapeptide revealed that none of their corresponding CD spectra match that of the Ni-GGNCC pentapeptide complex, indicating the Ni-pentapeptide complex does not undergo chiral inversion. NMR spectroscopy was employed for cross-validation. Differences are observed in the peptides synthesized to contain D amino acids in various positions, and the XXLLL GGNCC and the nickel-exposed GGNCC are nearly identical; thus, unlike the tripeptide system, chiral inversion does not occur in the pentapeptide system even in the presence of  $\text{O}_2$ .

In the Ni-NCC containing systems and the published maquettes of Ni-SOD, several characteristic reactivities have been noted. The Ni-NCC tripeptide complex is not able to bind a fifth ligand, have a measurable redox potential, or exhibit superoxide scavenging activity until site-specific chiral inversion has occurred. In contrast, even immediately after generation, the pentapeptides containing the NCC sequence exhibit all these features, suggesting access to the axial position is immediately available. Additionally, while the Ni-NCC complex is incredibly stable and does not undergo additional secondary reactions, the

Ni-GGNCC complex eventually loses color, likely as the result of as not yet identified, secondary chemistries. This is similar to the Ni-SOD maquettes, which have been noted to undergo thiol oxidation in the presence of oxygen. Indeed, the original Ni-SOD<sup>M1</sup> maquette decays over the course of hours to insoluble, high-molecular weight polymers when exposed to air.<sup>6</sup> DFT calculations and reactivity studies of synthetic complexes have suggested that bis-amide-ligated Ni<sup>II</sup> centers are even more unstable with respect to O<sub>2</sub>, being more prone to thiol oxidation than the corresponding amine/amide or bis-amine systems.<sup>19,21-23</sup> Thus, the decreased stability of the Ni-pentapeptides as compared to Ni-NCC is consistent with the change to bis-amide ligation for the former compounds. The extension of the sequence from NCC to GGNCC causes additional differences in the two peptides. The N-terminal amine that participates in binding nickel in the tripeptide is an amide in the pentapeptide. The difference between bis-amide and amine/amide coordination presumably alters the reactivity of the nickel(II) center with dioxygen, thereby preventing the occurrence of chiral inversion in the pentapeptide system. This lack of chiral inversion in the pentapeptide systems provides additional insight into the mechanism of chiral inversion within the Ni-NCC tripeptide system. The presence of oxygen promotes chiral inversion within the tripeptide; in the absence of oxygen, under an argon atmosphere, the LLL-Ni-NCC species is trapped.<sup>3</sup> In contrast, the Ni-GGNCC species remains as the XXLLL isoform, both in the presence and absence of oxygen. Because the addition of extra residues at the N-terminal end of the NCC sequence prevents chiral inversion, it is likely that the coordinated amine promotes reactivity in the first position in the NCC tripeptide, which then propagates, allowing chiral inversion at the third position. Both the chiral inversion and the superoxide scavenging chemistries rely heavily on the electronic environment around the metal center to accomplish electron transfer. The steric properties, however, may dictate the preferred electron transfer reaction pathway. For example, the chirally inverted tripeptide and the all-L tripeptide have the same primary ligands, but the dominant reaction with the all-L species is chiral inversion, whereas the Ni-pentapeptide species do not first undergo chiral rearrangement but instead immediately perform superoxide scavenging chemistry, like the inverted tripeptide. The chiral inversion alleviates strain, making the complex more planar, resulting in an extraordinarily stable DLD-tripeptide complex,<sup>2</sup> whereas the pentapeptide complexes subsequently undergo secondary reactions that have yet to be defined.

Comparison to the enzyme Ni-SOD and its maquettes provides insight into the function and unique reactivities of Ni-NCC. Ni-SOD is a complex enzyme with many factors governing its unique and efficient reactivity.<sup>11,12,24,25</sup> The presence of two cysteine ligands helps maintain the Ni<sup>II</sup>/Ni<sup>III</sup> redox couple that is necessary to catalyze the disproportionation reaction.<sup>26-29</sup> During catalysis, an axial histidine ligand is critical to stabilizing the nickel(III) oxidized state and helping to tune the nickel redox potential for superoxide disproportionation;<sup>12,13</sup> when the axial histidine is missing, the enzyme resides mostly in the nickel(II) (reduced) form, which decreases the rate of disproportionation by two orders of magnitude.<sup>24</sup> When the histidine in the peptide maquettes was replaced with noncoordinating residues, the superoxide scavenging activity dropped, emphasizing the importance of a fifth ligand.<sup>4</sup> The activity of the Ni-NCC containing peptides, which also lack a fifth ligand, is similar to these mutated maquettes. Although only a small paramagnetic component is detectable in the tripeptide, and MCD and EPR data suggest that no paramagnetic species accumulates in the pentapeptide, both the superoxide scavenging and chiral inversion chemistries likely rely on the ability of the NCC systems to access a nickel(III) state in order to facilitate electron transfer. CN<sup>-</sup> binding demonstrates a fifth ligand may access the axial position, but the lack of an internal ligand to help stabilize nickel(III) may make the nickel(III) state transient and undetectable in the NCC-containing peptides.

Other studies have probed the importance of the mixed amine/amide vs bis-amide coordination on the superoxide scavenging activity and redox potential; however, those studies were often complicated by the fact that the change from amine/amide to bis-amide ligation also resulted in a change in total charge of the compound (from  $-1$  to  $-2$  in the case of the Ni-SOD maquettes).<sup>5</sup> In contrast, Ni-NCC and the Ni-pentapeptides are both dianionic compounds.<sup>1,2,5,6</sup> Thus, these systems offer an opportunity to differentiate between the intrinsic effects of the amine/amide to bis-amide switch and those associated with the change in the charge of the complex. For example, when the maquette was acetylated to generate a bis-amide species, the redox potential shifted by  $-0.2$  V and superoxide scavenging activity decreased dramatically by over two orders of magnitude.<sup>5</sup> In contrast, the redox potentials and superoxide scavenging activities are very similar between the chirally inverted Ni-tripeptide and the Ni-pentapeptide, despite the differences in the primary coordination spheres. Thus, the overall charge of the complex, and not just the nature of the ligands, has a strong impact on these properties.

Despite much work in this area, the factors governing superoxide scavenging activity by Ni(II) complexes are still incompletely understood. For example, other maquettes have comparable SOD activities, but their redox potentials vary widely.<sup>4-6,9</sup> While synthetic complexes have been used to probe the chemistry and better understand how specific features of the enzyme facilitate catalysis, they often have measurable redox potentials but lack superoxide scavenging activity.<sup>14-17,30,31</sup> While Ni-GGNCC is a bis-amide complex that lacks a fifth ligand, Ni-NCC maintains the original amine/amide ligation yet lacks a fifth ligand, but both yield comparable activity to these modified maquettes. A bis-amide complex that lacks an internal fifth ligand has not yet been reported. Individually, removal of the axial histidine and acetylation to generate a bis-amide species significantly reduce the superoxide scavenging activity. Together these data suggest no simple correlation exists between ligand type, redox potential, and superoxide scavenging activity. Larger structural differences and the secondary coordination sphere further impact the reactivity with or without changing the redox potential, which make the enzyme much more efficient than small molecule mimics.<sup>11,12,10,13</sup> Taken with our data, the efficiency of the superoxide scavenging reaction also depends on the availability of alternative electron transfer pathways, in this case chiral inversion or degradation chemistries.

## Conclusions

In NCC-containing peptides, the presence of an amine in the first position results in the predominance of chiral inversion chemistry. Changing this moiety to an amide within GGNCC eliminates this electron transfer pathway, resulting in retention of the chirality and permitting immediate superoxide scavenging chemistry by the complex. Here we demonstrate that distinct reactions, specifically chiral inversion, superoxide scavenging activity, and degradation reactions, occur and are influenced by the moieties that coordinate the metal center within a series of NCC-containing peptides. While the electronic properties of the metal center must be conducive to perform electron transfer chemistry, the steric constraints contribute to the specificity of the reaction pathway.

## Supplementary Material

Refer to Web version on PubMed Central for supplementary material.

## Acknowledgments

We thank Emily Haynes for technical assistance, Dr. J. Douglas for assistance with NMR and EPR, Drs. C. Schöneich and O. Mozziconacci for insight into chiral peptide studies, Dr. K. Frankowski for assistance with IR, and Drs. S. Lunte, M. Hulvey, and C. Kuhnline for assistance with CV. This work was supported by the J. R. and

Inez Jay Fund (Higuchi Biosciences Center). M.E.K. was supported by the Madison and Lila Self Graduate Fellowship, the KU Cancer Center and the PhRMA Foundation Postdoctoral Fellowship in Pharmaceuticals. A.M.G. was supported by the NIH Dynamic Aspects of Chemical Biology Training Grant (T2 GM GM08454) and the NSF GK-12 Fellowship (0742523).

## References

- (1). Krause ME, Glass AM, Jackson TA, Laurence JS. *Inorg. Chem.* 2010; 49:362–364. [PubMed: 20000358]
- (2). Krause ME, Glass AM, Jackson TA, Laurence JS. *Inorg. Chem.* 2011; 50:2479–2487. [PubMed: 21280586]
- (3). Glass AM, Krause ME, Laurence JS, Jackson TA. *Inorg. Chem.* 2012; 51:10055–10063. [PubMed: 22928993]
- (4). Neupane KP, Gearty K, Francis A, Shearer J. *J. Am. Chem. Soc.* 2007; 129:14605–14618. [PubMed: 17985883]
- (5). Neupane KP, Shearer J. *Inorg. Chem.* 2006; 45:10552–10566. [PubMed: 17173410]
- (6). Shearer J, Long LM. *Inorg. Chem.* 2006; 45:2358–2360. [PubMed: 16529443]
- (7). Tietze D, Breitzke H, Imhof D, Koeth E, Weston J, Buntkowsky G. *Chemistry--A European Journal.* 2009; 15:517–523.
- (8). Tietze D, Tischler M, Voigt S, Imhof D, Ohlenschlaeger O, Goerlach M, Buntkowsky G. *Chemistry--A European Journal.* 2010; 16:7572–7578.
- (9). Shearer J, Neupane KP, Callan PE. *Inorg. Chem.* 2009; 48:10560–10571. [PubMed: 19894770]
- (10). Schmidt M, Zahn S, Carella M, Ohlenschlaeger O, Goerlach M, Kothe E, Weston J. *ChemBioChem.* 2008; 9:2135–2146. [PubMed: 18690655]
- (11). Wuerges J, Lee J-W, Yim Y-I, Yim H-S, Kang S-O, Carugo KD. *Proceedings of the National Academy of Sciences of the United States of America.* 2004; 101:8569–8574. [PubMed: 15173586]
- (12). Barondeau DP, Kassmann CJ, Bruns CK, Tainer JA, Getzoff ED. *Biochemistry.* 2004; 43:8038–8047. [PubMed: 15209499]
- (13). Herbst RW, Guce A, Bryngelson PA, Higgins KA, Ryan KC, Cabelli DE, Garman SC, Maroney MJ. *Biochemistry.* 2009; 48:3354–3369. [PubMed: 19183068]
- (14). Gale EM, Cowart DM, Scott RA, Harrop TC. *Inorg. Chem.* 2011; 50:10460–10471. [PubMed: 21932766]
- (15). Gale EM, Narendrapurapu BS, Simmonett AC, Henry F, Schaefer I, Harrop TC. *Inorg. Chem.* 2010; 49
- (16). Gale EM, Patra AK, Harrop TC. *Inorg. Chem.* 2009; 48:5620–5622. [PubMed: 20507097]
- (17). Gale EM, Simmonett AC, Telser J, Henry F, Schaefer I, Harrop TC. *Inorg. Chem.* 2011; 50:9216–9218. [PubMed: 21888395]
- (18). Shearer J, Zhao N. *Inorg. Chem.* 2006; 45:9637–9639. [PubMed: 17112256]
- (19). Mathrubootham V, Thomas J, Staples R, McCracken J, Shearer J, Hegg EL. *Inorg. Chem.* 2010; 49:5393–5406. [PubMed: 20507077]
- (20). Crapo JD, McCord JM, Fridovich I. *Methods Enzymol.* 1978; 53:382–393. [PubMed: 362127]
- (21). Grapperhaus CA, Mullins CS, Kozlowski PM, Mashuta MS. *Inorg. Chem.* 2004; 43:2859–2866. [PubMed: 15106973]
- (22). Hatlevik O, Blanksma MC, Mathrubootham V, Arif AM, Hegg EL. *J. Biol. Inorg. Chem.* 2004; 9:238–246. [PubMed: 14735332]
- (23). Grapperhaus CA, Darenbourg MY. *Acc. Chem. Res.* 1998; 31:451–459.
- (24). Bryngelson PA, Arobo SE, Pinkham JL, Cabelli DE, Maroney MJ. *J. Am. Chem. Soc.* 2004; 126:460–461. [PubMed: 14719931]
- (25). Choudhury SB, Lee J-W, Davidson G, Yim Y-I, Bose K, Sharma ML, Kang S-O, Cabelli DE, Maroney MJ. *Biochemistry.* 1999; 38:3744–3752. [PubMed: 10090763]
- (26). Johnson OE, Ryan KC, Maroney MJ, Brunold TC. *J Biol Inorg Chem.* 2010; 15:777–793. [PubMed: 20333422]

- (27). Ryan KC, Johnson OE, Cabelli DE, Brunold TC, Maroney MJ. *J Biol Inorg Chem*. 2010; 15:795–807. [PubMed: 20333421]
- (28). Bryngelson PA, Maroney MJ. *Metal Ions in Life Sciences*. 2007; 2:417–443.
- (29). Fiedler AT, Bryngelson PA, Maroney MJ, Brunold TC. *J. Am. Chem. Soc.* 2005; 127:5449–5462. [PubMed: 15826182]
- (30). Shearer J, Dehestani A, Abanda F. *Inorg. Chem.* 2008; 47:2649–2660. [PubMed: 18330983]
- (31). Lee W-Z, Chiang C-W, Lin T-H, Kuo T-S. *Chem. Eur. J.* 2012; 18:50–53. [PubMed: 22162207]

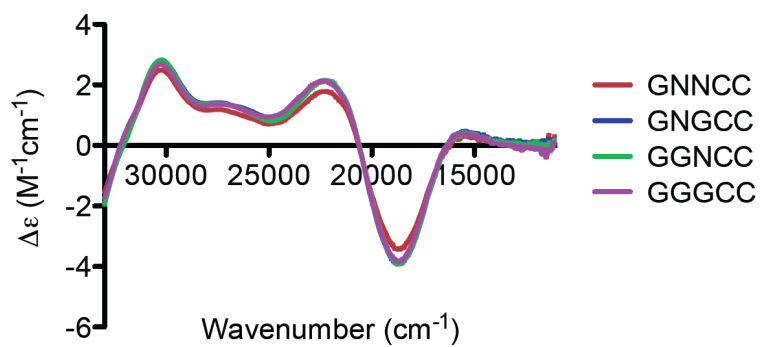


**Figure 1.** CD spectra of Ni-pentapeptides in 50 mM potassium phosphate pH 7.4, scanned 10 minutes after complex generation.

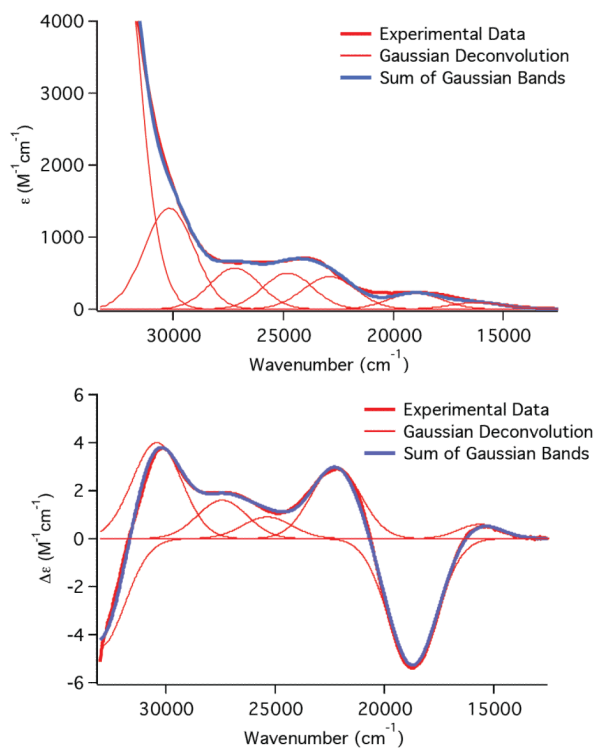


**Figure 2.** Gaussian deconvoluted absorption (top) and CD (bottom) spectra of Ni-GGNCC.

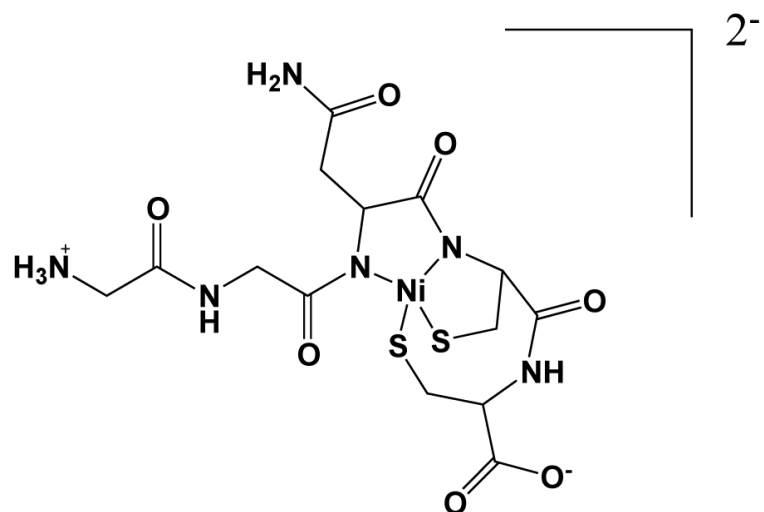


**Figure 3.**  
Structure of Ni-GGNCC showing bis-amide coordination.

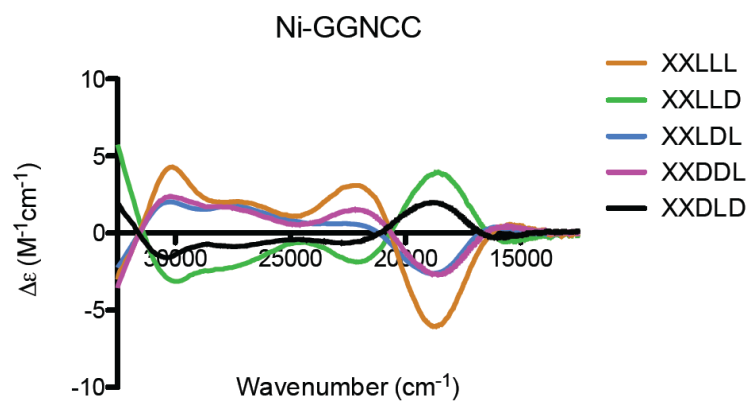


**Figure 4.**  
A. CD profiles of several chiral forms of GGNCC in phosphate buffer.

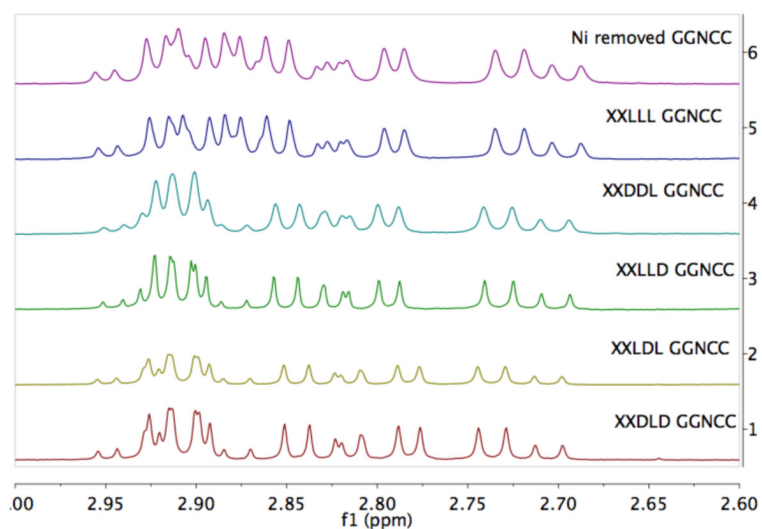


**Figure 5.** NMR spectra of Ni-exposed GGNCC compared to each D-containing form. Differences in splitting patterns between 2.6 and 3.0 ppm correspond to the different chiralities of the different pentapeptides.

Table 1

Energies of spectral bands in Ni-GGNCC compared to Ni-NCC.

| Ni-GGNCC                   |  |                            |  |                            |  | Ni-NCC <sup>a</sup>        |  |                            |  |                            |  |
|----------------------------|--|----------------------------|--|----------------------------|--|----------------------------|--|----------------------------|--|----------------------------|--|
| CD                         |  | Absorption                 |  | CD                         |  | Absorption                 |  | CD                         |  | Absorption                 |  |
| Energy (cm <sup>-1</sup> ) | $\Delta\epsilon$ (M <sup>-1</sup> cm <sup>-1</sup> ) | Energy (cm <sup>-1</sup> ) | $\epsilon$ (M <sup>-1</sup> cm <sup>-1</sup> ) | Energy (cm <sup>-1</sup> ) | $\Delta\epsilon$ (M <sup>-1</sup> cm <sup>-1</sup> ) | Energy (cm <sup>-1</sup> ) | $\epsilon$ (M <sup>-1</sup> cm <sup>-1</sup> ) | Energy (cm <sup>-1</sup> ) | $\Delta\epsilon$ (M <sup>-1</sup> cm <sup>-1</sup> ) | Energy (cm <sup>-1</sup> ) | $\epsilon$ (M <sup>-1</sup> cm <sup>-1</sup> ) |
| 15 600                     | 0.6  | 16 200                     | 90   | 14 000                     | -0.2   | 13 900                     | 160  | 16 270                     | -0.7   | 16 270                     | 290  |
| 18 700                     | -5.3   | 19 000                     | 220  | 18 730                     | 0.9  | 19 050                     | 570  | 21 550                     | 2.18   | 21 550                     | 930  |
| 22 200                     | 3  | 22 900                     | 450  | 21 600                     | 0.9  | 24 440                     | 1200   | 26 525                     | 3.1  | 26 525                     | 1400   |
| 25 350                     | 0.9  | 24 800                     | 500  | 24 350                     | 0.9  | 29 000                     | 1930   | 31 800                     | -1.4   | 31 900                     | 2530   |
| 27 410                     | 1.6  | 27 400                     | 570  | 26 200                     | 3.1  | 28 800                     | 1400   |                            |  |                            |  |
| 30 400                     | 4  | 30 220                     | 1400   | 6900 <sup>b</sup>          |  |                            |  |                            |  |                            |  |
| 33 000                     | -4.5   | 32 900                     | 6900 <sup>b</sup>                              |                            |  |                            |  |                            |  |                            |  |

<sup>a</sup>The Gaussian deconvolution of Ni<sup>II</sup>-NCC was performed using electronic absorption and CD data collected for this sample prepared under an Ar atmosphere. As described in reference 3, Ni<sup>II</sup>-NCC reacts rapidly with O<sub>2</sub> to initiate chiral inversion. Thus, the original electronic absorption and CD data reported for Ni<sup>II</sup>-NCC are not reflective of authentic Ni<sup>II</sup>-NCC.

<sup>b</sup>The extinction coefficient for this absorption band is determined by fitting the onset of absorption intensity in the near-UV region and thus is an approximate value.

**Table 2**

Coordination of  $\text{CN}^-$  to different nickel species, showing that  $\text{CN}^-$  coordinates to the pentapeptide immediately after generation, whereas with the tripeptide, chiral inversion must occur before a fifth ligand can bind. NCC and GGNCC samples were examined in potassium phosphate buffer at pH 7.4.

| Species  | $\nu(\text{C}\equiv\text{N})$ ( $\text{cm}^{-1}$ ) |
|--|--|
| KCN  | 2076   |
| $\text{K}_2[\text{Ni}(\text{CN})_4]^{7-}$                          | 2123   |
| $\text{Ni}(\text{CN})-(\text{mSOD})^{7-}$                          | 2108   |
| Ni-NCC + $\text{CN}^-$<br>(fresh) <sup>2</sup>                     | N/A  |
| Ni-NCC + $\text{CN}^-$<br>(aged—chirally<br>inverted) <sup>2</sup> | 2107   |
| Ni-GGNCC + $\text{CN}^-$<br>(fresh)                                | 2113   |